# AUTOMATIC MODULATION CLASSIFIER FOR MILITARY APPLICATIONS

*Víctor Iglesias, Jesús Grajal and Omar Yeste-Ojeda*

GMR-SSR, ETSI Telecomunicación, Universidad Politécnica de Madrid
30 Av. Complutense, 28040, Madrid, Spain
email: {viglesias, jesus, omar}@gmr.ssr.upm.es
web: www.gmr.ssr.upm.es

## ABSTRACT

Automatic modulation recognition plays an important role in several military and civilian applications. Depending on the application, latency can be the bottleneck for designing an automatic modulation classifier (AMC). In this paper, an AMC based on low complexity signal features to improve latency and percentage of real-time operation is designed for broad-band military applications.

## 1. INTRODUCTION

Automatic modulation classification of a signal is an intermediate operation between signal detection and data demodulation or system reaction (Electronic Warfare, EW). It plays a key task in several civilian and military receivers. Signal classification increases its difficulty without previous knowledge of the received data, symbol timing, carrier frequency, phase offsets, bandwidth, etc.

An AMC can be divided into two different sections [1]: signal preprocessing and the classification algorithm. The first section can estimates the signal power, signal to noise ratio, time of arrival, pulse width or carrier frequency. The optimum strategy is a joint design of these two sections. If this is not possible, the classification algorithm must be adapted to the estimation accuracies of signal preprocessing. Depending on the complexity of the AMC, it can be "real-time" or "off-line".

There are two groups of classification algorithms, likelihood-based (LB) [1,2] (also known as decision-theoretic) and feature-based (FB) approach (or pattern recognition approach) [1, 3–7]. The first group is based on the likelihood function of the received signal and the solution is optimal in the sense that it maximizes the probability of classification. The implementation of a likelihood-based algorithm requires high computational complexity and usually it is simplified into a suboptimal algorithm.

On the other hand, the FB algorithms extract several signal features and the classification is carried out by processing these features in a pre-designed way. The feature-based approaches are not optimal but are simpler to implement.

EW equipments should be capable of detecting, locating and identifying enemy signals in the minimum time in order to generate effective jamming responses or countermeasures. In that scenario, latency is one of the main problems for designing an AMC, so classification algorithm should be as simple as possible.

We have designed an FB AMC for military applications based on features of the instantaneous phase of the received signal. The modulation classification is based on a hierarchical decision tree. A signal is classified into 4 possible modulations: No Modulation (NM), Linear Frequency Modulation (LFM), Non-Linear Frequency Modulation (FM) and Phase Shift Keying (PSK). After this classification, PSK modulations are subclassified as 2PSK, 4PSK or MPSK (M > 4).

Partly supported by TEC2008-02148/TEC.

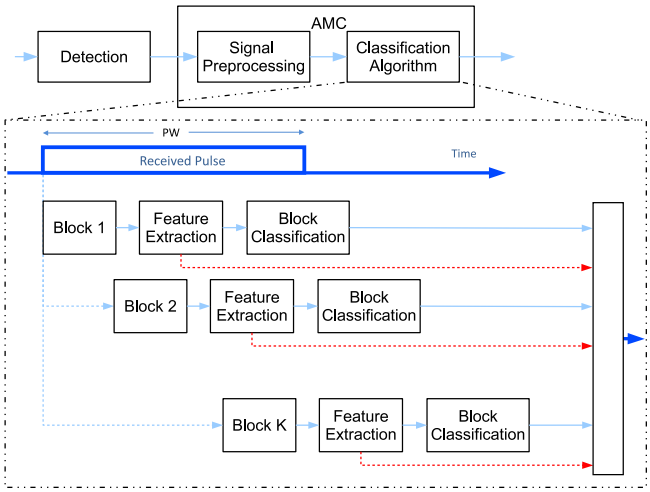


Figure 1: Global classification scheme. The block-by-block scheme reduces the computational complexity.

Modulation parameters such as chirp rate, bandwidth or symbol rate are estimated too.

## 2. GLOBAL CLASSIFICATION ALGORITHM

Once the signal is detected, its time of arrival (TOA) and pulse width (PW) are estimated (Figure 1). The carrier frequency is estimated too and the signal is converted to baseband, with a residual frequency error.

The input signal (PW samples) is divided into blocks of $N$ samples in order to reduce the computational complexity. The AMC works on a block-by-block scheme. Signal features are extracted for each block and the blocks are classified afterwards (Figure 1).

$N$ is fixed by the hardware implementation of the algorithm and by operational requirements like latency. For example, in a FPGA platform implementation, $N$ is limited by FPGA accumulators [7].

After the block-by-block operation, the AMC provides the final signal modulation and parameter estimates by collecting all the partial classifications and estimates. Several strategies can be applied. The one proposed consists of a priority system and a majority rule. The final classification is:

- NM if all the block classifications are NM.
- LFM if the majority of blocks are LFM, disregarding the blocks classified as NM.
- FM if the majority of blocks are FM, disregarding the blocks classified as NM.
- PSK if the majority of blocks are PSK, disregarding the blocks classified as NM.

Once the signal is classified as PSK, the modulation is:

- 2PSK if all the block classifications are 2PSK.

 

- 4PSK if all the blocks are classified as 2PSK or 4PSK.
- MPSK (M > 4) if at least one block is classified as MPSK.

## 3. BLOCK CLASSIFICATION ALGORITHM

The first step is to determine the signal features of interest. We have studied several signals features based on the unwrapped instantaneous phase and the normalized instantaneous frequency of the signal. The unwrapped instantaneous phase is calculated as follows:

$$\phi_u[n] = F_U(\phi[n]) \tag{1}$$

where $\phi[n]$ is the instantaneous phase and $F_U(\cdot)$ is the unwrap function.

The normalized instantaneous frequency is calculated as the first difference of the instantaneous phase divided by $2\pi$:

$$f_i[n] = \frac{\phi_u[n] - \phi_u[n-1]}{2\pi} \tag{2}$$

### 3.1 Signal features

The signal features extracted are:

- The mean square error (MSE) between the unwrapped phase and its least squares linear fitting:

$$\gamma_{NM} = \frac{1}{N}\sum_{n=0}^{N-1}\left(\phi_u[n] - a_{NM}\, n - b_{NM}\right)^2 \tag{3}$$

  where $a_{NM}$ and $b_{NM}$ are the coefficients of the linear fitting.
- The MSE between the unwrapped phase and its least squares parabolic fitting:

$$\gamma_{LFM} = \frac{1}{N}\sum_{n=0}^{N-1}\left(\phi_u[n] - a_{LFM}\, n^2 - b_{LFM} n - c_{LFM}\right)^2 \tag{4}$$

  where $a_{LFM}$, $b_{LFM}$ and $c_{LFM}$ are the coefficients of the parabolic fitting.
- The variance of the instantaneous frequency:

$$\gamma_V = \frac{1}{N-1}\sum_{n=1}^{N-1}\left(f_i[n] - \widehat{\mu}_{fi}\right)^2 \tag{5}$$

  where $\widehat{\mu}_{fi}$ is the estimated mean of $f_i[n]$.
- The kurtosis of the instantaneous frequency:

$$\gamma_K = \frac{1}{\gamma_V^2}\frac{1}{N-1}\sum_{n=1}^{N-1}\left(f_i[n] - \widehat{\mu}_{fi}\right)^4 \tag{6}$$

The signal features for the PSK subclassification are:

- The MSE between the unwrapped phase (previously multiplied by 2), $\phi_{u,2}[n]$, and its least squares linear fitting:

$$\gamma_{2\text{PSK}} = \frac{1}{N}\sum_{n=0}^{N-1}\left(\phi_{u,2}[n] - a_{2\text{PSK}}\, n - b_{2\text{PSK}}\right)^2 \tag{7}$$

  where $a_{2\text{PSK}}$ and $b_{2\text{PSK}}$ are the coefficients of the linear fitting.
- The MSE between the unwrapped phase (previously multiplied by 4), $\phi_{u,4}[n]$, and its least squares linear fitting:

$$\gamma_{4\text{PSK}} = \frac{1}{N}\sum_{n=0}^{N-1}\left(\phi_{u,4}[n] - a_{4\text{PSK}}\, n - b_{4\text{PSK}}\right)^2 \tag{8}$$

  where $a_{4\text{PSK}}$ and $b_{4\text{PSK}}$ are the coefficients of the linear fitting.

All signal features are selected because of its low complexity and the possibility of selecting SNR-independent thresholds, assuming an operational degradation.

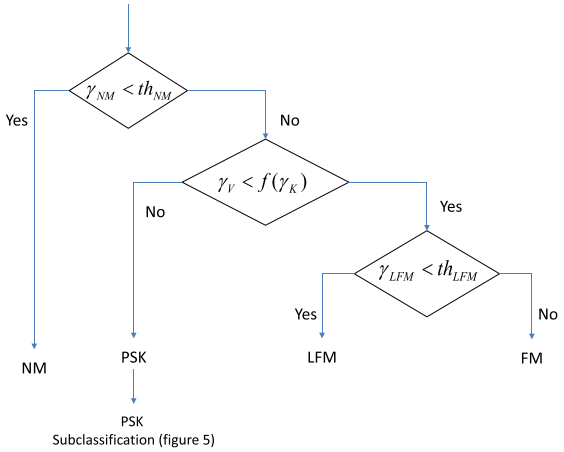


Figure 2: Hierarchical decision tree.

### 3.2 NM, PSK, LFM, FM classification

After the feature extraction, block classification is made following the hierarchical decision tree shown in Figure 2.

- Step 1. The unwrapped instantaneous phase of a NM signal is $\phi_u[n] = 2\pi f_c n$, where $f_c$ is the residual carrier frequency error. So, the first decision of the tree is (Figure 3):

$$\gamma_{NM} \underset{\text{NM}}{\gtrless} th_{NM} \tag{9}$$

- Step 2. The phase transitions of a PSK signal generate high spikes in the instantaneous frequency. In that case, the kurtosis of $f_i[n]$ for a PSK is greater than the kurtosis for the rest of modulations. The $\gamma_K - \gamma_V$ plane (variance - kurtosis of instantaneous frequency) is used to separate PSK signals (Figure 4):

$$\gamma_V \underset{\text{PSK}}{\lessgtr} f(\gamma_K) \tag{10}$$

  where $f(x)$ defines the decision region. We have adopted a linear region in logarithmical units, so the function is $f(x) = ax^b$.
- Step 3. If the instantaneous frequency of a LFM signal is a straight line, then the unwrapped instantaneous phase follows a parabolic equation (Figure 3). The final decision of the tree is:

$$\gamma_{LFM} \underset{\text{LFM}}{\overset{\text{FM}}{\gtrless}} th_{LFM} \tag{11}$$

### 3.3 PSK subclassification

If the signal is classified as PSK, the PSK subclassification is performed according to the hierarchical tree of Figure 5.

- Step 1. If the instantaneous phase of a 2PSK signal is multiplied by 2, phase transitions of $\pi$ are converted to $2\pi$ and then these phase transitions are eliminated by the unwrap function. In this case, the unwrapped instantaneous phase is a straight line and the first decision is (Figure 6):

$$\gamma_{2\text{PSK}} \underset{\text{2PSK}}{\gtrless} th_{2\text{PSK}} \tag{12}$$

- Step 2. Similarly to 2PSK, if the modulation is 4PSK then the instantaneous phase multiplied by 4 and unwrapped must be a straight line (Figure 6):

$$\gamma_{4\text{PSK}} \underset{\text{4PSK}}{\overset{\text{MPSK}}{\gtrless}} th_{4\text{PSK}} \tag{13}$$

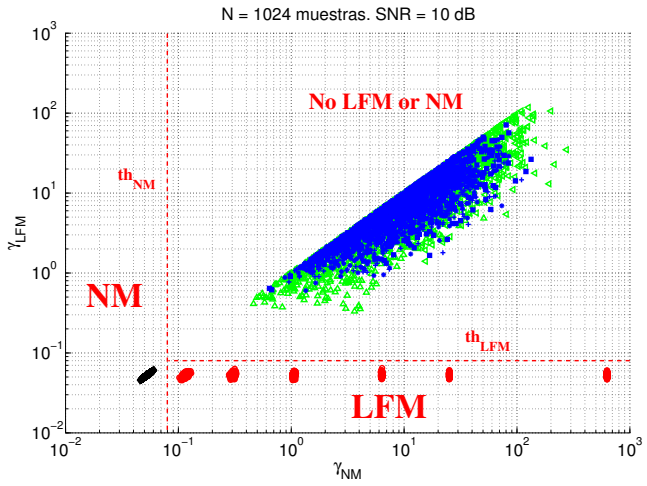


Figure 3: $\gamma_{NM} - \gamma_{LFM}$ plane. $N = 1024$, SNR = 10 dB. LFM - red circle, 2FSK - green triangle, 2PSK - blue square, 4PSK - blue cross, 8PSK - blue asterisk, NM - black diamond.

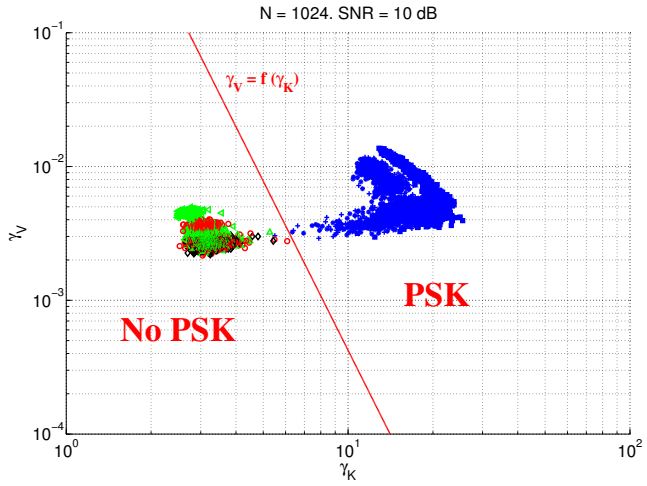


Figure 4: $\gamma_K - \gamma_V$ plane. $N = 1024$, SNR = 10 dB. LFM - red circle, 2FSK - green triangle, 2PSK - blue square, 4PSK - blue cross, 8PSK - blue asterisk, NM - black diamond.

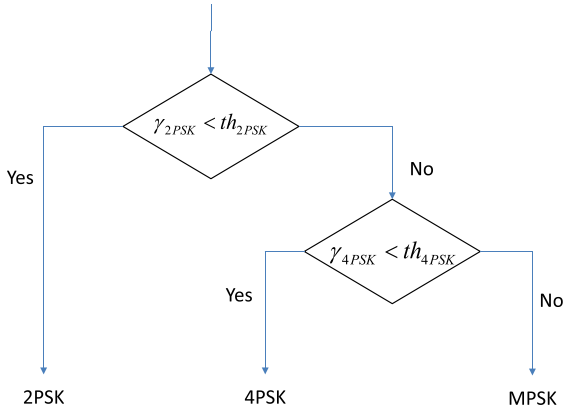


Figure 5: Hierarchical decision tree for PSK subclassification.

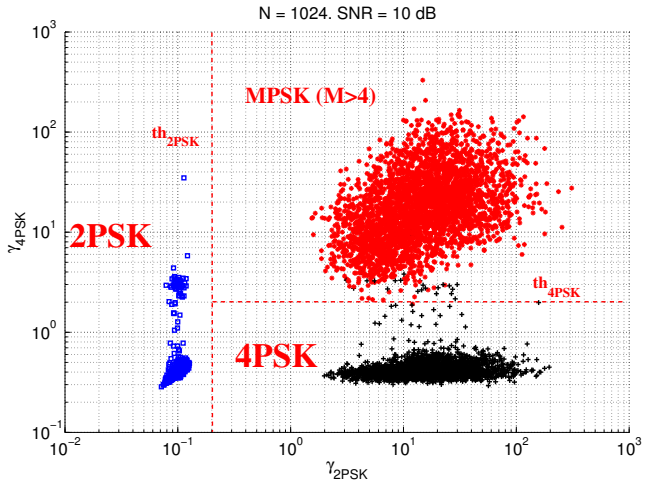


Figure 6: $\gamma_{2\text{PSK}} - \gamma_{4\text{PSK}}$ plane. $N = 1024$, SNR = 10 dB. 2PSK - blue square, 4PSK - black cross, 8PSK - red asterisk.

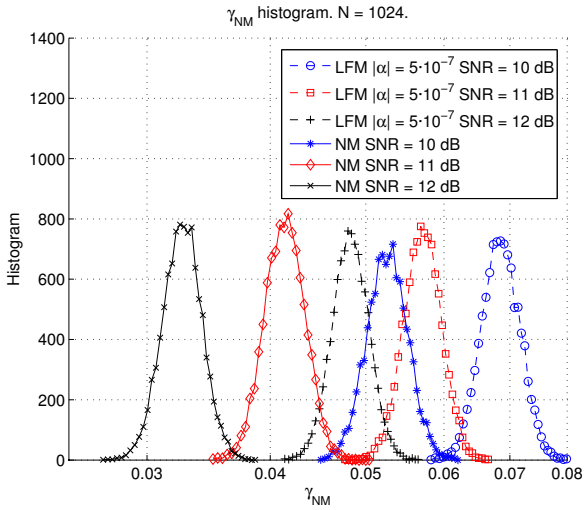


Figure 7: $\gamma_{NM}$ histogram of NM and LFM signal.

Computational burden of some features could be reduced decimating the unwrapped instantaneous phase. In that case, feature variances increase and thresholds should be modified.

## 4. THRESHOLD IMPLEMENTATION

AMC performance is analyzed with complex signals corrupted with Complex Additive White Gaussian Noise (C-AWGN). Block length is $N = 1024$ samples. Signal frequencies and bandwidths are normalized by sampling frequency and LFM chirp rates ($\alpha$) are normalized by the square of sampling frequency. Residual carrier frequency error follows a continuous uniform distribution between $-4 \cdot 10^{-3}$ and $4 \cdot 10^{-3}$.

Thresholds $th_{NM}$, $f(x)$, $th_{LFM}$, $th_{2\text{PSK}}$ and $th_{4\text{PSK}}$ are calculated with Monte Carlo simulations for a wide range of modulations and SNR. Thresholds can be selected either dependent or independent of SNR. If SNR is not estimated, thresholds should be fixed for an objective SNR, resulting in an additional performance degradation for higher SNR, as is justified in the following example.

Figure 7 shows the histogram of $\gamma_{NM}$ for NM and LFM ($|\alpha| = 5 \cdot 10^{-7}$ and $|\alpha| = 2 \cdot 10^{-6}$) and SNR = 10, 11 and 12 dB. Separation between NM and LFM increases with

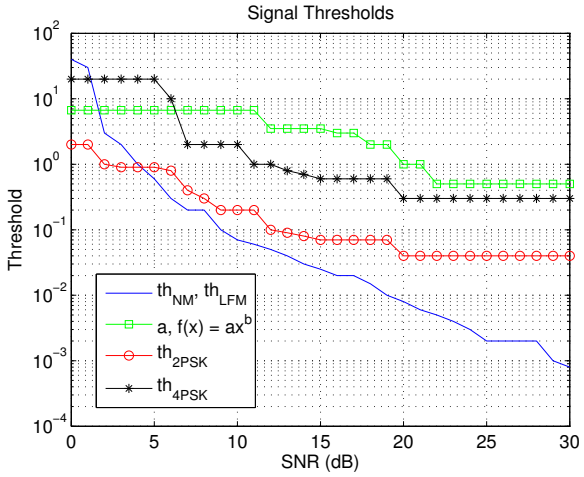


Figure 8: $th_{NM} = th_{LFM}$, $a$ $(f(x))$, $th_{2\text{PSK}}$ and $th_{4\text{PSK}}$ variation with SNR. $b = -4.7$ is SNR-independent in $f(x)$.

Table 1: Confusion matrix. LFM signal, $N = 1024$. SNR-dependent thresholds ($\sigma = 0$ dB, known SNR).

| SNR = 10 dB | LFM | NM |
|---|---|---|
| $\|\alpha\| = 5 \cdot 10^{-7}$, PW = 1400 | 0 | 100 |
| $\|\alpha\| = 1 \cdot 10^{-6}$, PW = 1400 | 100 | 0 |
| SNR = 12 dB | LFM | NM |
| $\|\alpha\| = 5 \cdot 10^{-7}$, PW = 1400 | 28 | 72 |
| $\|\alpha\| = 5 \cdot 10^{-7}$, PW = 3500 | 44 | 56 |
| $\|\alpha\| = 5 \cdot 10^{-7}$, PW = 7000 | 84 | 16 |

SNR but signal histograms move slightly to the left. If thresholds are SNR-independent and optimized for SNR = 10 dB, LFM signal with $|\alpha| = 5 \cdot 10^{-7}$ will be classified as NM for SNR = 11 and 12 dB. This is a consequence of NM being an LFM signal with $\alpha = 0$. As is shown in section 5, LFM signals with higher $|\alpha|$ are classified correctly.

Figure 8 shows the calculated thresholds as a function of SNR. These thresholds have been obtained by maximizing the joint probability of correct classification for the different groups of signals defined at each branch of the decision tree (Figure 2 and 5). As is shown in Figure 8, thresholds decrease with SNR.

When thresholds are SNR-dependent, the error in the estimate of SNR is modeled by a gaussian random variable with zero mean and $\sigma$ (dB) standard deviation.

## 5. PRACTICAL RESULTS

Global AMC performance depends on block length ($N$), the pulse width (PW), the combination of the different block classifications to provide a final signal modulation and the threshold implementation. Classification performance improves with $N$. Experimental results point out that below SNR = 5 dB signal classification performance is very poor because the instantaneous phase is unwrapped incorrectly. SNR required for detection is lower than SNR for classification and at the same time SNR needed for classification is lower than SNR for demodulation. The main conclusions of AMC performance are summarized next.

First of all, LFM classification depends basically on the chirp rate magnitude. Slow LFM signals will be classified as NM. Tables 1 and 2 show the confusion matrix for 100 Monte Carlo trials and various LFM signals. The probability of correct classification (CCP) increases with $|\alpha|$ and PW,

Table 2: Confusion matrix. LFM signal, PW = 3500 samples, $N = 1024$. SNR-dependent ($\sigma = 0$ dB, known SNR) vs. SNR-independent (fixed for SNR = 10 dB) thresholds.

| $\|\alpha\| = 1 \cdot 10^{-6}$, SNR (dB) | Independent | | Dependent | |
|---|---|---|---|---|
| | LFM | NM | LFM | NM |
| 10 - 16 | 100 | 0 | 100 | 0 |
| 18 | 96 | 4 | 100 | 0 |
| 20 | 7 | 93 | 100 | 0 |
| $\|\alpha\| = 2 \cdot 10^{-6}$, SNR (dB) | Independent | | Dependent | |
| | LFM | NM | LFM | NM |
| 10 - 16 | 100 | 0 | 100 | 0 |
| 18 | 100 | 0 | 100 | 0 |
| 20 | 100 | 0 | 100 | 0 |

Table 3: Confusion matrix. 2FSK signal, SNR = 8 dB, $\Delta f = 0.5/T_s$, $N = 1024$. SNR-dependent thresholds ($\sigma = 0$ dB, known SNR).

| SNR = 8 dB, $\Delta f = 0.5/T_s$ | LFM | FM | PSK | NM |
|---|---|---|---|---|
| $T_s = 350$, PW = 3500 | 4 | 94 | 2 | 0 |
| $T_s = 350$, PW = 7000 | 0 | 99 | 1 | 0 |
| $T_s = 230$, PW = 3500 | 0 | 99 | 1 | 0 |
| $T_s = 230$, PW = 7000 | 0 | 100 | 0 | 0 |

Table 1. In Table 2 an example of SNR-independent and SNR-dependent thresholds is shown. When SNR increases, LFM signal is classified from LFM to NM because thresholds are fixed for SNR = 10 dB.

Concerning FM classification, it depends mainly on signal bandwidth. For example, 2FSK signal classification is influenced by symbol rate, frequency separation and the number of symbols. Table 3 shows the confusion matrix for 100 Monte Carlo trials and several 2FSK signals. $T_s$ is the number of samples per symbol and $\Delta f$ is the frequency separation. Increasing 2FSK symbol rate and pulse width improves the probability of correct classification.

PSK classification is affected by the number and magnitude of phase transitions that generate high spikes in the instantaneous frequency. 2PSK signals are easier to classify than other PSK because all its frequency spikes are $\pm 0.5$. Table 4 presents the confusion matrix for different PSK modulations. It is shown that classification enhances with symbol rate for a fixed SNR.

Finally, PSK subclassification also depends on

Table 4: Confusion matrix. PSK signals, $N = 1024$, PW = 3500. SNR-dependent thresholds ($\sigma = 0$ dB, known SNR).

| | SNR = 10 dB | | SNR = 16 dB | |
|---|---|---|---|---|
| | FM | PSK | FM | PSK |
| 2PSK, $T_s = 350$ | 0 | 100 | 0 | 100 |
| 4PSK, $T_s = 350$ | 18 | 82 | 1 | 99 |
| 8PSK, $T_s = 350$ | 22 | 78 | 2 | 98 |
| | SNR = 10 dB | | SNR = 12 dB | |
| | FM | PSK | FM | PSK |
| 2PSK, $T_s = 140$ | 0 | 100 | 0 | 100 |
| 4PSK, $T_s = 140$ | 7 | 93 | 0 | 100 |
| 8PSK, $T_s = 140$ | 8 | 92 | 0 | 100 |

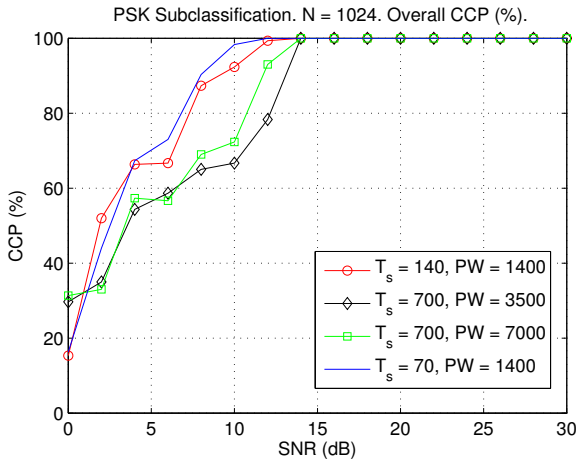


Figure 9: PSK subclassification.

symbol rate and pulse width. Figure 9 shows the overall CCP for PSK subclassification, defined as CCP = (Prob{2PSK|2PSK} + Prob{4PSK|4PSK} + Prob{MPSK|8PSK})/3. Overall CCP improves with symbol rate and pulse width. Like other PSK classification algorithms [1], separation between 4PSK and higher order MPSK requires more SNR than classification between 2PSK and 4PSK to achieve an objective CCP.

Table 5 presents the sensitivity ($S$, dB) for various modulations, defined as the SNR value for which the CCP is higher than 90 %. PW = 7000 and 2FSK frequency separation is $\Delta f = 0.5/T_s$. "NC" means that signal CCP does not tend to 100 % for high SNR, as it was shown on Table 1. Thresholds in first, second and third columns are SNR-dependent and SNR error estimation depends on standard deviation $\sigma$. In fourth column, thresholds are SNR-independent and optimized for an objective SNR of 10 dB. Table 5 shows a performance degradation with $\sigma$ for signals close to thresholds (Figure 8). On the other hand, when thresholds are SNR-independent, operational degradation is not significant except for low chirp rate LFM and narrow bandwidth 2FSK.

Other AMCs [6, 7] present better sensitivity due to the processing gain of channelization, but CCP is poor for signals with high instantaneous bandwidth. The algorithm in [3] has better performance, but it is much more complex with at least 10 signal features and a neural network based classifier.

## 6. CONCLUSION

We have designed a feature-based Automatic Modulation Classifier for military applications. The AMC works in a block-by-block basis. Signal features are extracted for each block and then the block is classified following a hierarchical decision tree. A final decision is taken by processing all the partial classifications. Signal classification depends on block length and signal parameters. The introduction of SNR-dependent thresholds improves signal classification. When SNR is estimated, degradation is significative for signals whose features are close to thresholds.

The main achievement of the proposed AMC resides in the low complexity of the feature extraction and the decision tree, allowing implementation with low latency and high percentage of real time. Currently, this AMC is being implemented in a FPGA platform.

Table 5: Sensitivity ($S$ dB), CCP = 90%. CCP is Prob{LFM|LFM}, Prob{FM|2FSK}, Prob{PSK|2PSK}, Prob{PSK|4PSK}, Prob{PSK|8PSK} and Prob{NM|NM}. $\sigma$, standard deviation of SNR estimation. $N$ = 1024, PW = 7000. "NC", "Not Classified". 100 Monte Carlo trials.

| $S$ (dB) | Threshold Implementation | | | |
|---|---|---|---|---|
| | $\sigma = 0$ | $\sigma = 0.5$ | $\sigma = 1$ | Fixed |
| LFM, $\lvert\alpha\rvert = 2 \cdot 10^{-7}$ | 22 | 24 | 29 | NC |
| LFM, $\lvert\alpha\rvert = 5 \cdot 10^{-7}$ | 13 | 16 | 20 | NC |
| LFM, $\lvert\alpha\rvert = 1 \cdot 10^{-6}$ | 10 | 10 | 14 | NC |
| LFM, $\lvert\alpha\rvert \geq 2 \cdot 10^{-6}$ | 7 | 8 | 10 | 10 |
| 2FSK, $T_s = 1400$ | 11 | 14 | 18 | NC |
| 2FSK, $T_s = 700$ | 10 | 10 | 13 | NC |
| 2FSK, $T_s = 350$ | 7 | 7 | 8 | 8 |
| 2FSK, $T_s \leq 140$ | 6 | 6 | 7 | 7 |
| 2PSK, $T_s = 1400$ | 11 | 12 | 12 | 12 |
| 4PSK, $T_s = 1400$ | 17 | 17 | 18 | 19 |
| 8PSK, $T_s = 1400$ | 20 | 21 | 22 | 22 |
| 2PSK, $T_s = 700$ | 10 | 10 | 11 | 10 |
| 4PSK, $T_s = 700$ | 16 | 16 | 17 | 18 |
| 8PSK, $T_s = 700$ | 17 | 17 | 17 | 18 |
| 2PSK, $T_s = 140$ | 7 | 8 | 8 | 8 |
| 4PSK, $T_s = 140$ | 10 | 10 | 10 | 10 |
| 8PSK, $T_s = 140$ | 10 | 11 | 12 | 12 |
| 2PSK, $7 \leq T_s \leq 70$ | 7 | 7 | 7 | 7 |
| 4PSK, $7 \leq T_s \leq 70$ | 8 | 8 | 8 | 8 |
| 8PSK, $7 \leq T_s \leq 70$ | 8 | 8 | 9 | 9 |
| NM | 8 | 8 | 8 | 10 |

## REFERENCES


[1] O. A. Dobre, A. Abdi, Y. Bar-Ness, and W. Su, "Survey of automatic modulation classification techniques: classical approaches and new trends", *Communications, IET*, vol. 1, no. 2, pp. 137–156, 2007.

[2] J. L. Xu, W. Su and M. Zhou, "Likelihood-Ratio Approaches to Automatic Modulation Classification", Accepted for inclusion in *Systems, Man, and Cybernetics, Part C: Applications and Reviews, IEEE Transactions on*.

[3] J. Lundén and V. Koivunen, "Automatic Radar Waveform Recognition", *IEEE Journal of Selected Topics in Signal Processing*, vol. 1, no. 1, pp. 124–136, 2007.

[4] A. K. Nandi and E. E. Azzouz, "Algorithms for Automatic Modulation Recognition of Communication Signals", *Communications, IEEE Transactions on*, vol. 46, no. 4, pp. 431–436, 1998.

[5] E. E. Azzouz and A. K. Nandi, "Procedure for automatic recognition of analogue and digital modulations", *Communications, IEE Proceedings*, vol. 143, no. 5, pp. 259–266, 1996.

[6] G. López-Risueño, J. Grajal, and A. Sanz, "Digital channelized receiver based on time-frequency analysis for signal interception", *Aerospace and Electronic Systems, IEEE Transactions on*, vol. 41, no. 3, pp. 879–898, 2005.

[7] J. Grajal, O. Yeste-Ojeda, M. A. Sánchez, M. Garrido and M. López-Vallejo, "Real Time FPGA Implementation of an Automatic Modulation Classifier for Electronic Warfare Applications", Accepted for inclusion in the *2011 European Signal Processing Conference (EUSIPCO-2011)*.